# DEVELOPMENT OF 1.3 GHz CAVITY COMBINER FOR 24 kW CW SSA*

W. Liu, G.R. Huang†, L.Shang, H.X. Lin, B.T. Du, W.B. Song
NSRL, University of Science and Technology of China, Hefei, CHINA

*Abstract*

The 24 kW CW SSA (Solid-State Amplifier) is being developed to drive the 1.3 GHz SC Linac used in a THz light source. The SSA adopts the compact all-in-one combining method – cavity combiner, which is proposed and developed in recent years [1]. This paper reports the R&D of the cavity combiner. The cavity combiner resonates in TM010 mode, coupling with 24 coaxial-connected 1 kW amplifier modules. The cavity's electromagnetic characteristic is calculated, and the mechanical structure including the input and output coupler has been designed.

## PRINCIPLE OF CAVITY COMBINER

The resonant cavity can be equivalent to an RLC parallel resonant circuit. In practical applications, the resonator is often coupled with two external transmission systems. One system contains power and the other is connected to the load. Assuming that both of them are matched, the equivalent circuit is shown in Fig. 1. It can be simplified as shown in Fig. 2.

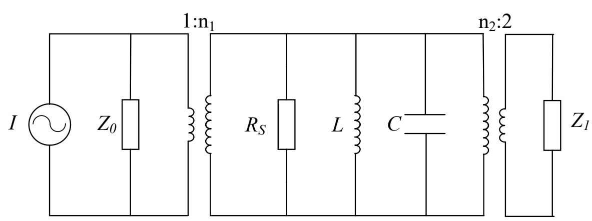


Figure 1: Equivalent circuit.

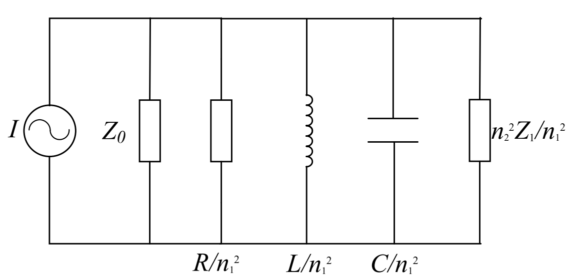


Figure 2: Simplified equivalent circuit.

The power losses in the resonant cavity is $P_d = n_1^2V^2/2R$, in the system containing power is $P_{e1} = V^2/2Z_0$, in the other is $P_{e2} = V^2/2Z_1$. Total loss is $P = P_d + P_{e1} + P_{e2}$. The power stored in the resonator is $W = n_1^2CV^2/2$. It can derivate the following formulas about Q-factor.

$$Q_0 = \omega_0 W/P_d = \omega_0 RC$$

$$Q_{e1} = \omega_0 W/P_{e1} = \omega_0 n_1^2 Z_0 C$$

$$Q_{e2} = \omega_0 W/P_{e2} = \omega_0 n_2^2 Z_1 C$$

$$Q_L = \omega_0 W/P$$

$$\frac{1}{Q_L} = \frac{1}{Q_0} + \frac{1}{Q_{e1}} + \frac{1}{Q_{e2}}$$

The coupling coefficients between the resonator and the two systems are defined respectively.

$$\beta_1 = \frac{P_{e1}}{P_d} = \frac{Q_0}{Q_{e1}}, \beta_2 = \frac{P_{e2}}{P_d} = \frac{Q_0}{Q_{e2}}$$

The reflection coefficient of this system is

$$\Gamma_1 = \frac{\beta_1 - \beta_2 - 1}{1 + \beta_1 + \beta_2}$$

The condition of the resonant cavity that matches the system that contains the power is $\Gamma_1 = 0$. So, the relations of the two coupling coefficients can be expressed as $\beta_1 = 1 + \beta_2$. Similarly, an n-port cavity combiner can be equivalent to a resonator coupled to n identical input couplers and an output coupler. The equivalent circuits are shown in Fig. 3 and Fig. 4. The condition of matching is $\beta_0 = n\beta_i + 1$.

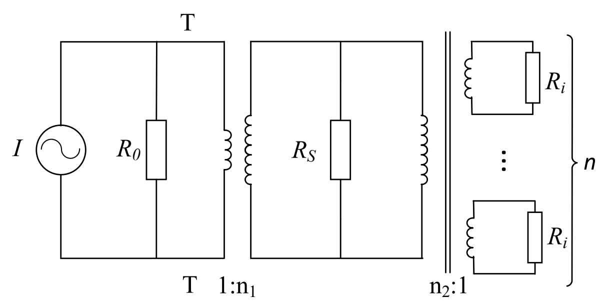


Figure 3: Equivalent circuit.

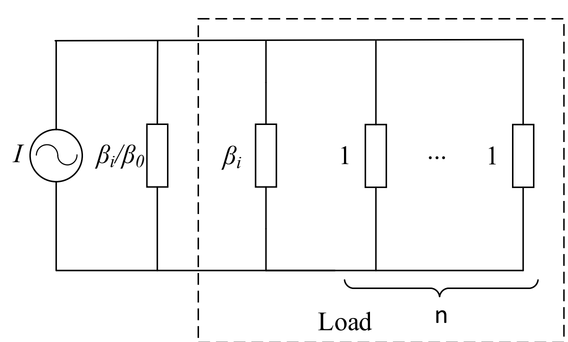


Figure 4: Equivalent circuit.

## DESIGN METHOD

The relation of the output power $P_0$ and cavity power loss $P_d$ is $\beta_0 = P_0/P_d$. The power loss ratio can be expressed as $\eta_l = P_d/P_0 = 1/\beta_0$. The cavity combiner resonates in TM010 mode, coupling with 24 coaxial-connected 1 kW amplifier modules. In view of TM010 mode electromagnetic field characteristics, the input cou-

* Supported by National Natural Science Foundation of China (No.21327901).
email: grhuang@ustc.edu.cn

pler coupling method using ring coupling. The power loss ratio $\eta_l$ is about 2% when $\beta_i = 2$. The loss power is about 0.5 kW. In this case, the normal cooling method can ensure that the resonator is working properly. We replaced the cylindrical resonator with eight-prism. Output coupler adopts hard coaxial line.

## DESIGN RESULTS

The whole design process is divided into the following five parts, cavity, input coupler, output coupler, output waveguide and tuning.

### *Cavity*

Although the eight prism and cylinder are different, but basically similar, we can use the theory of cylindrical resonator to design an eight-prism resonator [1]. In the cylindrical resonator the radius of the cavity is

$$a = \frac{c}{2.62f}$$

The results of simulation are listed in Table 1 and Table 2. The TM010 electric and magnetic fields is shown in Fig. 5.

Table 1: Cavity Parameters

| Name | Value(mm) | Description |
|---|---|---|
| r_cavity | 93.4 | cavity radius |
| l_cavity | 300 | cavity length |
| h_wall | 13 | cavity wall thickness |

Table 2: Modes

| Number | Frequency |
|---|---|
| 1 | 1.108332 |
| 2 | 1.301243 |
| 3 | 1.393782 |

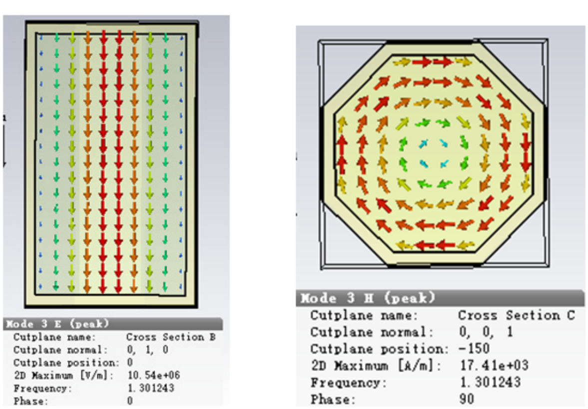


Figure 5: TM010 electric and magnetic fields.

The frequency difference between TM010 and upper and lower modes is about 200 MHz and 90 MHz, respectively.

### *Input Coupler*

The size of the input coupler is obtained by simulations. The parameters and the construction of the input coupler are shown in Table 3 and Fig. 6. The coupling coefficient is about 2.04 for this size.

Table 3: Input Coupler Parameters

| Name | Value(mm) | Description |
|---|---|---|
| r_incoupler | 5 | bend radius |
| l_incoupler | 5 | extension length |
| r_in_1 | 1 | conductor radius |

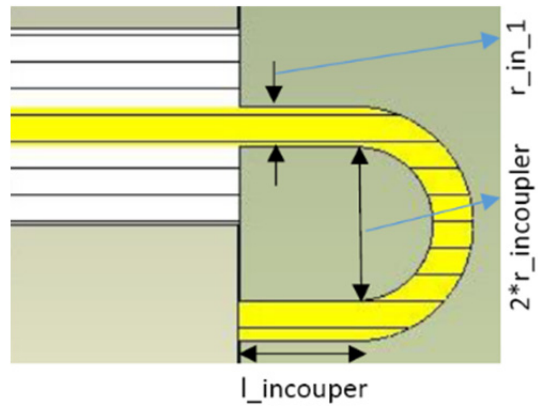


Figure 6: Input coupler.

### *Output Coupler*

The output coupler uses a hard-coaxial line of 50-35 model. The parameters and the construction of the output coupler are shown in Table 4 and Fig. 7.

Table 4: Output Coupler Parameters

| Name | Value(mm) | Description |
|---|---|---|
| l_outcoupler_in | 5 | extension length |
| l_outcoupler_up | 15 | stretched length |
| l_connector | 25 | connector length |

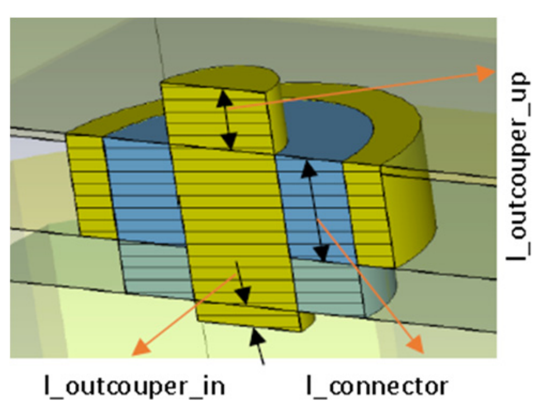


Figure 7: Output coupler.




ISBN 978-3-95450-182-3

### *Output Waveguide*

The transmission system uses the rectangular waveguide of the BJ14 model. One end of the waveguide is a removable short-circuit board. The output coupling coefficient can be changed by changing the position of the short-circuit board. The variation of output coupling coefficient with short-circuit board is shown in Fig. 8.

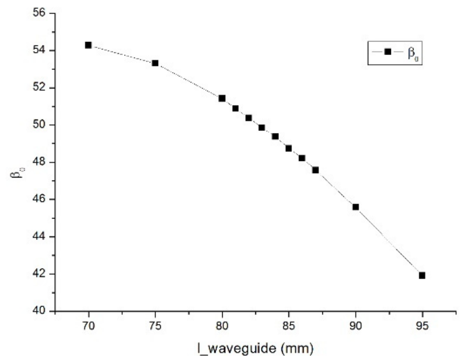


Figure 8: The variation of output coupling coefficient with short-circuit board.

The input coupling coefficient $\beta_i$ is 2.04. The output coupling coefficient $\beta_0$ is about 50 by matching conditions $\beta_0 = n\beta_i + 1$. So, the short-circuit board position is about 83 mm.

### *Tuning*

The resonant frequency can be changed by input coupler, output coupler and output waveguide. So we need the tuning rod to adjust the resonant frequency. The length of the tuning rod is negatively correlated with the resonant frequency. The parameters and the construction of the tuning are shown in Table 5 and Fig. 9.

Table 5: Tuning Parameters

| Name | Value(mm) | Description |
|---|---|---|
| l_tuning | 5 | tuning length |
| r_tuning | 10 | tuning radius |

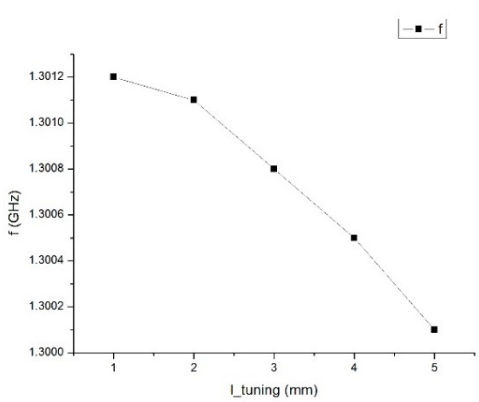


Figure 9: The variation of resonant frequency with tuning length.

## SIMULATION RESULTS

Set the waveguide output port to 1 port and the input coupler ports to 2-25. The 1 port is power source to simulate the calculation of S-parameters. The simulation results about S-parameters and 3 dB bandwidth are shown in Fig. 10 and Fig. 11.

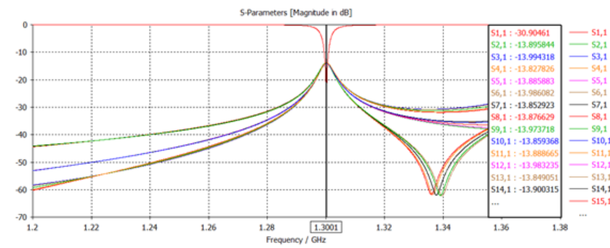


Figure 10: S-Parameters.

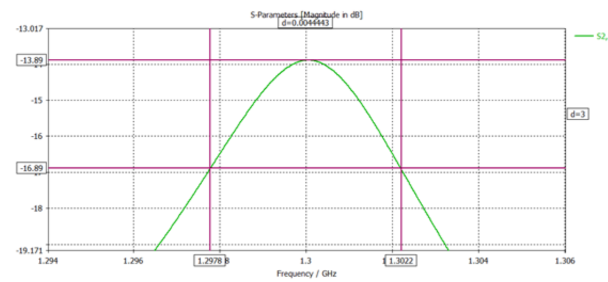


Figure 11: 3 dB bandwidth of the S21.

The S11 is -30.90461 dB, which shows that the power reflection coefficient between the resonant cavity and the output waveguide is very small when the frequency is 1.3 GHz. The difference between the maximum and minimum values of Sn1 is 0.166 dB, and the maximum phase difference for each port is 2.47 degrees. It indicates that the power transfer of each input branch is very consistent. The half-power bandwidth of the cavity combiner is equal to the 3 dB bandwidth of the S21. The 3 dB bandwidth of S21 is 4.4 MHz in the simulation results [3].

## CONCLUSION

Based on the equivalent principle of cavity combiner, the relationship between input and output coupling coefficient and loss rate is obtained, and a design method of cavity combiner is proposed. We completed the 1.3 GHz cavity combiner design work and simulation work, next to complete the prototype manufacturing and RF test work.

## REFERENCES

[1] J. Jacob, *et al.*, "Commissioning of First 352.2 MHz - 150 kW Solid State Amplifiers at the ESRF and Status of R&D", in *Proc. IPAC'13*, pp. 2708-2710, WEPFI004

[2] W.X. Wang, *Microwave Engineering Technology*. National Defense Industry Press, 2014, pp. 281-282

[3] David M. Pozar, *Microwave Engineering*. John Wiley & Sons, Inc Press, 2012.